IOP PUBLISHING JOURNAL OF PHYSICS G: NUCLEAR AND PARTICLE PHYSICS

J. Phys. G: Nucl. Part. Phys. **39** (2012) 124001 (16pp) doi:10.1088/0954-3899/39/12/124001

Renormalizing the double-beta operator for the shell model

Jonathan Engel

Department of Physics and Astronomy, CB3255, University of North Carolina, Chapel Hill, NC 27599-3255, USA

E-mail: engelj@physics.unc.edu

Received 9 June 2012
Published 19 November 2012
Online at stacks.iop.org/JPhysG/39/124001

Abstract

We review work, much of it by the author and collaborators, to take omitted levels into account in shell-model calculations of neutrinoless double-beta decay. Previous work on this type of problem deals mainly with corrections to the shell-model Hamiltonian. Here we focus on corrections to the two-body transition operator that governs the rate of neutrinoless decay. Corrections in the form of two-body effective operators appear to be significant but have yet to be fully pinned down. Three-body effective operators may be significant as well.

(Some figures may appear in colour only in the online journal)

1. Introduction

Unlike some approaches to the nuclear many-body problem, the nuclear shell-model contains a clearly-defined truncation scheme that makes successively better approximations to an exact solution of the many-body problem straightforward, at least in principle. Other methods that have been applied to double-beta ($\beta\beta$) decay are harder to connect with exact calculations. The quasiparticle random-phase approximation (QRPA) makes the assumption that excited states are vibrations, a step that limits the scope of higher-order approximations. Energy-density functional theory starts from a mean-field framework that allows improvements to a point but still cannot be convincingly connected to a more fundamental framework. The interacting boson model (IBM) is, roughly speaking, an approximation to a very-large-scale shell model that neglects all but the most collective degrees of freedom.

The shell model is different, consisting essentially of an adjustable and straightforward truncation of the many-nucleon Hilbert space. As the space is enlarged the shell model approaches the no-core shell model, an ab initio method that is capable in principle of producing essentially exact results. The simplicity of the approximation scheme long ago prompted the development of techniques to compensate for the truncation by modifying the shell-model Hamiltonian and transition operators. The techniques are difficult to apply in

a completely faithful way and have often been mixed with phenomenology. Nevertheless, a framework exists that connects effective shell-model interactions and operators with the underlying bare interactions and operators, in principle completely.

Many more people have worked on Hamiltonians, however, than on transition operators and there is essentially no work on two-body transition operators. In neutrinoless double-beta ($0\nu\beta\beta$) decay we are faced with a two-body operator that changes charge, which, needless to say, nobody has considered before. What appears here is therefore as much a preview as a review; we discuss the preliminary work—mostly by the author and collaborators—on effective $0\nu\beta\beta$ operators for the shell model and outline promising avenues for future research.

2. Theoretical framework

2.1. Phenomenology

Modern shell-model and QRPA interactions are currently derived approximately from the bare nucleon–nucleon interaction, with careful adjustments made to reproduce spectra and transitions. The phenomenology underlying the shell-model double-beta transition operators is much cruder. In two-neutrino ($2\nu\beta\beta$) decay, which consists of successive single-beta decays to virtual intermediate-nucleus states, the axial-vector coupling constant g_A is often renormalized by a factor of about $1/1.26$. The renormalization reflects the empirical damping of Gamow–Teller strength that presumably comes from complicated nuclear correlations not included in state-of-the-art calculations and/or from many-body currents. Whether the same value for g_A is appropriate for $0\nu\beta\beta$ decay, which receives contributions not only from virtual Gamow–Teller transitions to states with $J^\pi = 1^+$ but also from nonzero-momentum-transfer transitions to states with higher angular momentum, is an open question. In any event, the use of $g_A \approx 1$ is the only modification to the bare operator, apart from an explicit treatment of short-range correlations, that people generally make.

2.2. Operator definitions

In the impulse approximation for the weak current and the closure approximation for the sum over intermediate states (which has been shown to be quite good), the $0\nu\beta\beta$ transition rate, can be related to the matrix element of a two-body operator:

$$\mathcal{M}_{fi} \equiv \langle f| \sum_{ab} M^{0\nu}_{ab} |i\rangle \equiv \langle f| \sum_{ab} M^{\rm GT}_{ab} + M^{F}_{ab} + M^{T}_{ab} |i\rangle \,. \tag{1}$$

The last term above is a very small tensor piece [1] that will be ignored here. The other two are given by [1, 2]

$$\begin{aligned} M^{\rm GT}_{ab} &= H_{\rm GT}(r_{ab})\, \boldsymbol{\sigma}_a \cdot \boldsymbol{\sigma}_b\, \tau^+_a \tau^+_b \\ M^{F}_{ab} &= H_{F}(r_{ab})\, \tau^+_a \tau^+_b, \end{aligned} \tag{2}$$

with the labels a and b indicating nucleons both here and in (1), r_{ab} representing internucleon distance, and the 'neutrino potentials' H defined by

$$H_K(r) = \frac{2R}{\pi r} \int_0^\infty \frac{h_K(q) \sin qr}{q + \bar{\omega}}\, {\rm d}q, \quad K = GT, F. \tag{3}$$

The quantity $\bar{\omega}$ in (3) is an average intermediate-nucleus excitation energy to which the H_K are not very sensitive. The $h_K(q)$ contain g_A as well as form factors that account for the finite size of the nucleon, and the effects of forbidden currents.

Adjusting the value of g_A simply means multiplying $M^{\rm GT}_{ab}$ by a constant. The incompleteness of nuclear models surely requires a more refined renormalization than that.

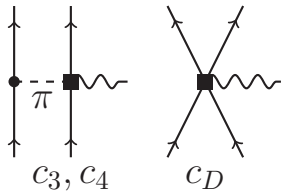

Figure 1. Chiral-EFT diagrams generating a two-body contribution to the weak current. The wiggly line represents the current and the dashed line the exchange of a pion.

This review will focus on nuclear-structure corrections to the effective operator, but it is important first to note another source: two-body contributions to the 'bare' beta-decay operator. Such contributions, traditionally treated via meson exchange models, are now handled more rigorously [3] in chiral effective field theory (EFT). They are represented by the diagrams in figure 1; each of the coefficients c_3, c_4, and c_D appear in the three-body part of the chiral-EFT interaction as well as in the two-body currents, and so can be constrained by binding energies and spectroscopy.

Reference [3] finds that these two-body corrections to the usual weak current, resulting in three-body corrections to the $\beta\beta$ operators in (2), can alter $0\nu\beta\beta$ matrix elements by up to 35%. Much of the g_A renormalization just mentioned may be due to these bare many-body currents. To keep matters simple we will not include such currents here, but the size of the effects they might generate should be kept in mind.

2.3. Lee–Suzuki mapping

To discuss effective interactions and operators in the shell model one needs to define a shell-model space, which we will sometimes call the 'small space', with some dimension d. One typically selects d eigenvectors of the full Hamiltonian in the full many-body harmonic-oscillator Hilbert space (of which the shell-model space is a small part) and then applies a Lee–Suzuki mapping [4, 5], which goes as follows: one lets P project onto the small d-dimensional shell-model space (usually consisting of valence particles in at most a single shell), with $|p\rangle$ denoting states that are entirely in that space and $|q\rangle$ states that are entirely outside. The d orthogonal small-space states $|\tilde{k}\rangle$ corresponding to the d selected full-space eigenstates $|k\rangle$ are defined by

$$|\tilde{k}\rangle \equiv M^{-\frac{1}{2}}(P+\omega^\dagger)\,|k\rangle\,, \tag{4}$$

with

$$\begin{aligned}\langle q|\,\omega\,|p\rangle &= \sum_{k=0}^{d-1}\langle q|k\rangle\,\langle \underline{k}|p\rangle \\ \langle p|\,\omega\,|q\rangle &= \langle q|\,\omega\,|q\rangle = \langle p|\,\omega\,|p\rangle = 0.\end{aligned} \tag{5}$$

and

$$M = P + \omega^\dagger\omega = P\big(1+\omega^\dagger\omega\big)P. \tag{6}$$

In (5) the $\langle \underline{k}|p\rangle$ are the elements of the inverse of the dimension-d matrix with elements $\langle p|k\rangle$. The shell-model effective operator $O_{\rm eff}$, be it Hamiltonian or decay operator[1], that gives the same matrix elements as the operator O in the d selected full-space states is then

$$O_{\rm eff} = M^{-\frac{1}{2}}(P+\omega^{\dagger})O(P+\omega)M^{-\frac{1}{2}}. \tag{7}$$

The matrix elements of $O_{\rm eff}$ can be written explicitly as

$$\langle p|\, O_{\rm eff}\, |p'\rangle = \sum_{p_1,p_2,k,k'=0}^{d-1} \langle p|\, M^{-\frac{1}{2}}\, |p_1\rangle\, \langle p_1|\underline{k}\rangle\, \langle k|\, O\, |k'\rangle\, \langle \underline{k}'|p_2\rangle\, \langle p_2|\, M^{-\frac{1}{2}}\, |p'\rangle, \tag{8}$$

where the elements of M can be written in the same fashion as

$$\langle p|\, M\, |p'\rangle = \sum_{k=0}^{d-1} \langle p|\underline{k}\rangle\, \langle \underline{k}|p'\rangle. \tag{9}$$

One can most easily apply these mappings to generate effective operators for systems with two particles in the valence shell. Of course the nuclei that undergo double-beta decay usually have many valence nucleons, but the effective two-nucleon operators should be a good starting point. Three-nucleon operators are under exploration and the size of their effects will be discussed later from several points of view.

3. Perturbation theory

One way to evaluate the effective interaction and decay operator of (7), followed in [6], is through diagrammatic perturbation theory. The lowest-order approximation (yielding bare operators) is to neglect ω in (7). Then, though the approach is formulated in a different language (see, e.g., [7]), and the question of applying the matrix M above is complicated [8], ω is effectively expanded in powers of the 'G matrix.' That G-matrix is obtained by summing a series in the bare two-body interaction V, which in [6] was taken to be the Bonn-A potential [9]. Alternatively, one can use an effective low-momentum potential in place of the G matrix [10]. To fully include the effects of high-momentum states, however, one must construct a low-momentum decay operator as well. The ladder sum that defines the G matrix can also be applied to the decay operator and we describe that procedure now.

Figure 2 displays the diagrams that yield the G matrix. The energies of the railed lines that appear as intermediate states are restricted to be above the valence-shell energy by at least 10 or so oscillator $\hbar\omega$. The summation over all such graphs, accomplished by solving a Bethe–Goldstone equation, takes into account the hard core of the bare nucleon–nucleon interaction, replacing it with a better behaved interaction that is suitable for use in perturbation theory.

The same procedure can be applied to the $0\nu\beta\beta$ operator. Now the ladder graphs contain one insertion of a double-beta line among the ladder of potential lines from figure 2. The result is the series shown in figure 3. The figure contains some new features: the vertical red (solid) and blue (dotted) lines represent neutrons and protons, the thin dashed line labeled $\mathcal{M}$ is the bare $0\nu\beta\beta$ operator, which turns neutrons into protons, and $\mathcal{M}_{\rm high}$ is the $\beta\beta$ analogue of the G matrix that takes into account short-range (high-energy) correlations.

To see the effects of these short-range correlations, one folds the two-body matrix elements of $\mathcal{M}_{\rm high}$ with transition densities associated with a shell-model calculation. Figure 4 displays the results of that folding with transition densities from the calculation in [11] of the decay of

[1] We assume that isospin is conserved and that the charge changing effective decay operator one needs can thus be obtained easily from its charge-conserving counterpart in (7).

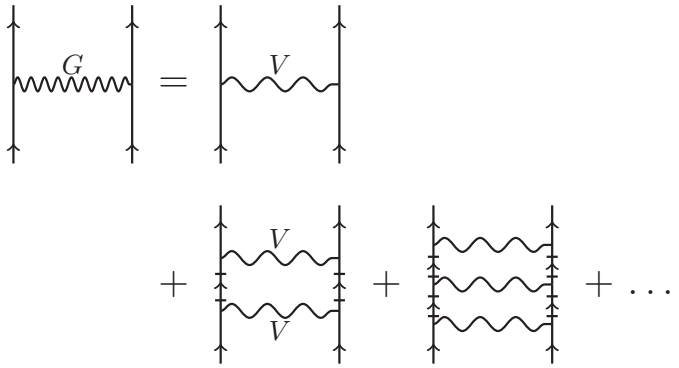

Figure 2. The diagrams generating the G matrix. Railed vertical lines are intermediate nucleons with very high energy. The mildly wiggly lines labelled V represent the bare interaction and the very wiggly line labelled G represents the G matrix.

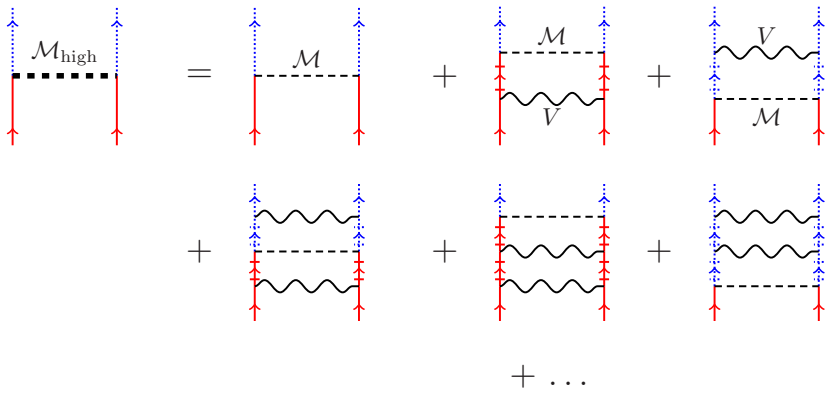

Figure 3. The diagrams generating $\mathcal{M}_{\rm high}$, the analogue of the G matrix. Solid (red) lines are protons, dotted (blue) lines neutrons and railed lines are intermediate nucleons at very high energy. The dashed horizontal line labeled $\mathcal{M}$ is the bare $0\nu\beta\beta$ operator and that labeled $\mathcal{M}_{\rm high}$ is the $0\nu\beta\beta$ operator that includes the effects of short-range correlations.

^{82}Se. The figure shows the contribution at each value of the internucleon separation r to $M_{\rm GT}$, the exact definition of which is

$$C^{\rm GT}(r) \equiv H_{\rm GT}(r)\,\langle f|\sum_{a<b}\delta(r-r_{ab})\boldsymbol{\sigma}_a\cdot\boldsymbol{\sigma}_b\tau_a^+\tau_b^+\,|i\rangle. \tag{10}$$

(The $H_{\rm GT}$ in the figure does not include the effects of nucleon from factors or forbidden currents.) The short-range correlations in $\mathcal{M}_{\rm high}$ push the contributions from small to intermediate values of the internucleon separation. The degree of displacement is less, however, than that induced by the phenomenological Jastrow function [12] traditionally used in calculations of double-beta decay and shown alongside the exact and ladder-based results in the figure. The ladder-sum, labeled 'microscopic correction,' is in quite good agreement with the results of the unitary correlator operator method (UCOM) [13–15].

Having obtained operators that include the effects of short-range correlations one can use the G matrix and $\mathcal{M}_{\rm high}$ to evaluate diagrammatic contributions to the full $0\nu\beta\beta$ matrix element that represent perturbation expansions in G. Reference [6] evaluated all such diagrams that

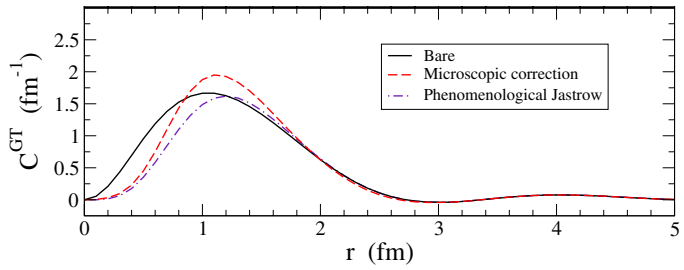

Figure 4. The contribution from each internucleon distance to the Gamow–Teller matrix element in (2) for the decay of ^{82}Se (with shell-model wavefunctions from [11]). The solid line (——) represents the contributions with no short-range corrections, the dashed red line (- - - -) represents the effects of the diagrams in figure 3, and the dash-dotted purple line (— · —) represents the effects of the phenomenological Jastrow function from [12].

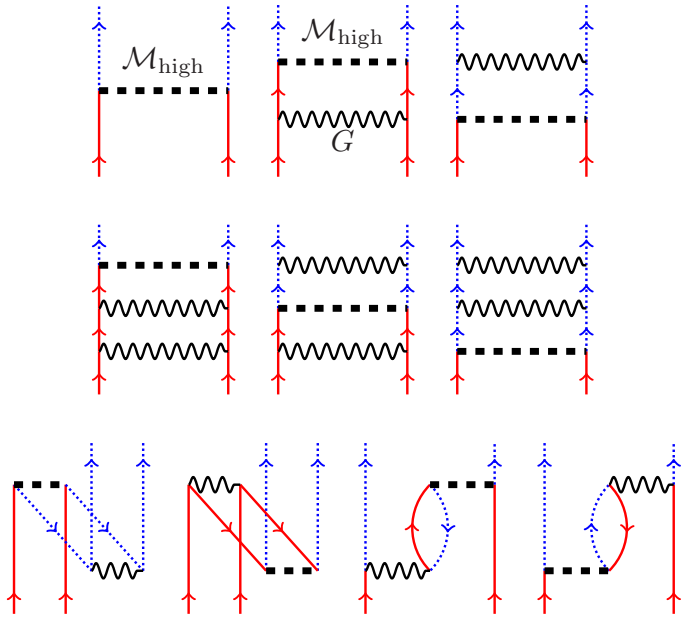

Figure 5. Perturbative contributions to the effective decay operator that are first-order in G, plus three ladder diagrams that are second-order in G. The lines have the same meaning as in earlier figures.

are first-order in G (not counting bubble insertions, which are neglected throughout this work despite the use an oscillator basis) and a few ladder diagrams of second-order. The diagrams appear in figure 5, with exchange diagrams implicitly included both here and later. After again combining the effective operator with the transition densities from [11] for ^{82}Se, the results for $M_{\rm GT}$ (without forbidden currents or nucleon form factors) are as follows: the bare matrix element is 3.33, the diagram on the top left gives 3.06 (quenched by short-range correlations as expected), summing all the diagrams except the last two on the bottom right raises the value to 5.39, and the last two diagrams, which represent core polarization by the interaction and $\beta\beta$ process, reduce it back to 3.25. This last number is nearly the same as the bare value, so that

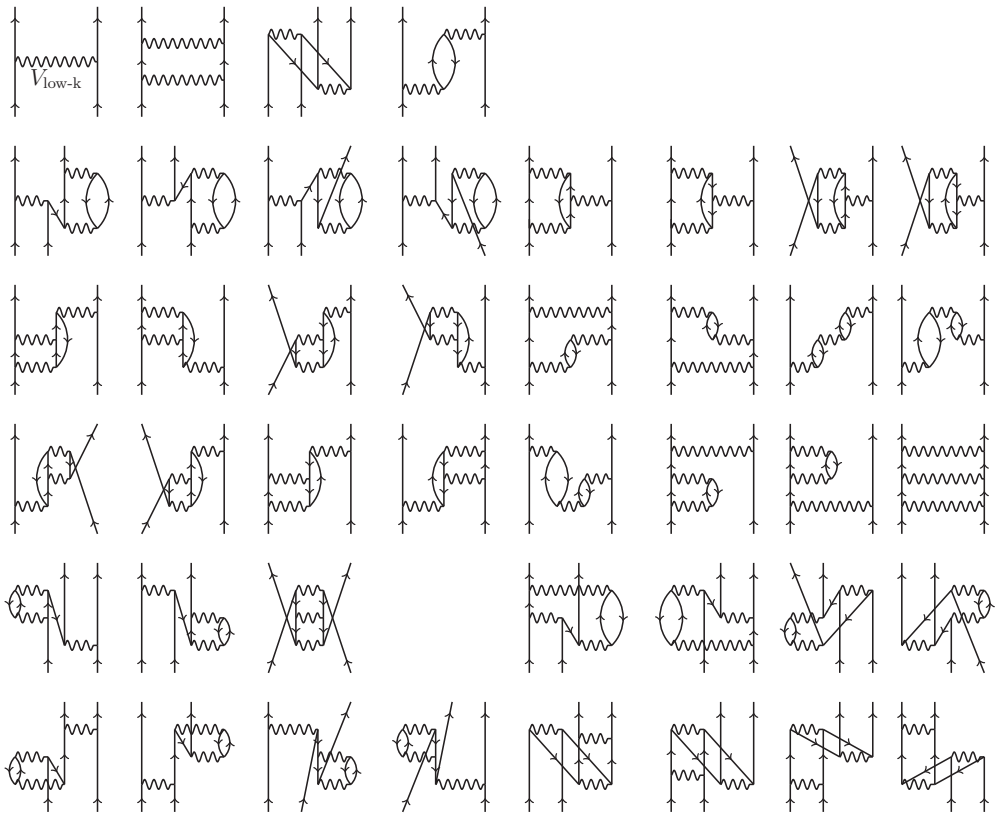

Figure 6. Diagrams in the expansion of the effective interaction defining the two-body part of the second- and third-order $\hat{Q}$-box (see text). The wiggly line now represents $V_{\text{low-k}}$ rather than the G matrix. We can obtain the first- and second-order '$\hat{X}$-box'—the set of all unfolded second-order diagrams for the effective operator (not including norm diagrams) modified by replacing one interaction in each of these diagrams by a $\beta\beta$ operator (in all possible ways) and restricting the sums over nucleons in the intermediate states to either neutrons or protons, as in the second-order diagrams in figure 5.

the net change is very small. The changes due to individual diagrams are substantial, however, so one cannot reasonably conclude that higher-order diagrams, including folded diagrams, will not have a significant effect. Three-and-more-body diagrams could contribute as well.

Diagrams that are second-order in the effective interaction and higher-order folded diagrams are in fact under investigation at present. Holt and Engel [16] are currently evaluating all the transition-matrix-element diagrams associated with the unfolded interaction diagrams shown in figure 6. The set includes diagrams that are both second- and third-order in the effective interaction; their $\beta\beta$ counterparts are first- and second-order. The wiggly interaction lines now represent the low-momentum interaction $V_{\text{low-k}}$, which often has better convergence properties rather than the G matrix used so far. Use of $V_{\text{low-k}}$ means that the kinds of diagrams in figure 3 leading to $\mathcal{M}_{\text{high}}$ cannot be included, but their effects can be accurately mocked up through the effective Jastrow function given in [17]. In addition, the diagrams in the figure represent only the effective interaction at third-order; to get the effective $\beta\beta$ operator at second-order one must substitute a dashed $\beta\beta$ line for each interaction line in each of the diagrams shown and colour the nucleon lines red or blue accordingly. (The resulting set contains so many

diagrams that we don't show it here). Finally, folded diagrams and corrections to state norms must be included. References [18] and [19] show that these additions amount to the following. Call the sum of the unfolded interaction diagrams (such as the third-order contributions to the two-body part in figure 6) the 'Q-box' $\hat{Q}(\varepsilon)$ and the corresponding sum of effective-$\beta\beta$-operator diagrams the 'X-box' $\hat{X}(\varepsilon_i, \varepsilon_f)$. Here the energies refer to the unperturbed energies of the initial and final states (both of which we eventually set to a single value ε). Then the matrix representing the final effective operator is

$$\mathcal{M} = \left(1 + \frac{1}{2}\frac{\mathrm{d}\hat{Q}(\varepsilon)}{\mathrm{d}\varepsilon} + \cdots\right)\left[\hat{X}(\varepsilon) + \hat{Q}(\varepsilon)\frac{\partial\mathcal{M}(\varepsilon_f,\varepsilon)}{\partial\varepsilon_f}\bigg|_{\varepsilon_f=\varepsilon} + \frac{\partial\hat{X}(\varepsilon,\varepsilon_i)}{\partial\varepsilon_i}\bigg|_{\varepsilon_i=\varepsilon}\hat{Q}(\varepsilon) + \cdots\right] \times\left(1 + \frac{1}{2}\frac{\mathrm{d}\hat{Q}(\varepsilon)}{\mathrm{d}\varepsilon} + \cdots\right), \tag{11}$$

where the products represent matrix multiplication.

The terms in round parentheses in (11) represent state norms and those in square brackets the folding of the effective-operator diagrams. Were we to include the ellipses, diagrams beyond third-order, and three-and-higher body effective-operator diagrams, this expression would give the exact result (assuming convergence).

Preliminary calculations in the expanded framework just described—$\hat{Q}$-box to third-order in $V_{\text{low-k}}$, $\hat{X}$-box to second-order, norms and folding as indicated in (11), yield a matrix element that is about 30% larger than the shell-model result with the bare operator reported in [11], bringing the shell model closer to the QRPA. This result is significant but it is a little too early to declare it accurate and conclusive. The matrix element could still be modified by higher-order diagrams and, particularly, by many-body operators. In the next section we describe nonperturbative calculations in a schematic model and in light systems to get a handle on the likely size of the many-body corrections.

4. Nonperturbative approaches

4.1. Initial test in algebraic model

Reference [20] uses group-theoretic methods to construct the effective two-body decay operator in a model that includes proton–neutron pairing. Because this kind of study is unusual nowadays, we describe it in some detail here. The paper considers the transition ^{76}Ge to ^{76}Se in a 'small' space containing 12 protons and 24 neutrons (for Ge) in a degenerate $\mathrm{pfg}_{9/2}$ valence shell, and in a 'large' space containing the small space together with all possible excitations of the nucleons into a degenerate version of the next shell ($\mathrm{sdg}_{7/2}$), an energy ϵ (which can be varied) above the $\mathrm{pfg}_{9/2}$ shell. The single-particle wavefunctions come from a harmonic oscillator with length parameter $b = 2.12$ fm.

The Hamiltonian is constructed from pairing operators that generate the group $SO(5) \times SO(5)$ (one $SO(5)$ for each degenerate shell) [21]:

$$H = \epsilon\hat{N}_2 - G\sum_{a,b=1}^{2}\left(S^{\dagger a}_{pp}S^{b}_{pp} + S^{\dagger a}_{nn}S^{b}_{nn} + g_{pp}S^{\dagger a}_{pn}S^{b}_{pn} - g_{ph}\mathbf{T}_a\cdot\mathbf{T}_b\right) \tag{12}$$

where $a, b = 1, 2$ label the shells (lower and upper), ϵ is the energy difference between the shells, $\hat{N}_2$ is the number operator for the upper shell, $\mathbf{T}_a$ is total isospin operator for shell a, and

$$S^{\dagger a}_{pp} = \frac{1}{2}\sum_{\alpha\in a}\hat{j}_\alpha[\pi^\dagger_\alpha\pi^\dagger_\alpha]^0_0, \quad S^{\dagger a}_{nn} = \frac{1}{2}\sum_{\alpha\in a}\hat{j}_\alpha[\nu^\dagger_\alpha\nu^\dagger_\alpha]^0_0, \quad S^{\dagger a}_{pn} = \frac{1}{\sqrt{2}}\sum_{\alpha\in a}\hat{j}_\alpha[\pi^\dagger_\alpha\nu^\dagger_\alpha]^0_0. \tag{13}$$

Here $\pi^\dagger_\alpha$ ($\nu^\dagger_\alpha$) creates a proton (neutron) in level α with angular momentum j_α, $\hat{j} \equiv \sqrt{2j+1}$, and the square brackets indicate angular-momentum coupling. The algebra of $SO(5)$ contains the three pair-creation operators above (for a given set a of levels), three corresponding destruction operators, the three components of the isospin $\mathbf{T}_a$, and the number operator $\hat{N}_a$. Since H contains only generators of $SO(5) \times SO(5)$, its lowest lying eigenstates consist of configurations in which the nucleons are entirely bound in isovector S pairs of the type in (13).

The Hamiltonian above violates isospin (T) conservation unless $g_{pp} = 1$. The application of this model relies on an analogy between double Fermi decay, the 2ν version of which vanishes when isospin is exactly conserved, and double-Gamow–Teller decay in a more realistic model, the 2ν version of which vanishes when the isoscalar and isovector pairing are of roughly equal strength.

To calculate the Fermi matrix element, one uses a basis of fully-paired states labelled $|\mathcal{N}_1, T_1, M_1; \mathcal{N}_2, T_2, M_2\rangle$, where $\mathcal{N}_1$ refers to the number of pairs in level-set 1 (the $\mathrm{pfg}_{9/2}$ shell), T_1 to the isospin of those $\mathcal{N}_1$ pairs (with $\mathcal{N}_1 - T_1$ even), M_1 to the isospin projection of those pairs, etc, and $M_1 + M_2 = 1/2(Z-N)$. The Hamiltonian, (12), and 2ν decay Fermi decay operator, $\sum_{\alpha,\beta} \tau^+_\alpha \tau^+_\beta$ are products of generators and one can evaluate their matrix elements, which depend only on the quantum numbers of the pairs, following, e.g., [22]. But the 0ν operators contain position-dependent factors that do not belong to the algebra. Their matrix elements depend on the wavefunctions of the single-particle states that make up basis and require more effort to evaluate. They can be computed via the generalized Wigner–Eckart theorem [22], which for matrix elements of an operator $\mathcal{M}$ between fully paired states in $SO(5)$ is:

$$\begin{aligned}\langle \Omega_a, \mathcal{N}_a, T_a, M_a \big| \mathcal{M}^{(\omega_1,\omega_2)}_{\mathcal{N}_0,T_0,M_0} \big| \Omega_a, \mathcal{N}'_a, T'_a, M'_a \rangle &= \langle (\Omega_a, 0) \| \mathcal{M}^{(\omega_1,\omega_2)} \| (\Omega_a, 0) \rangle \\ &\times \langle T'_a M'_a; T_0 M_0 \mid T_a M_a \rangle \langle (\Omega_a, 0) \mathcal{N}'_a T'_a; (\omega_1, \omega_2) \mathcal{N}_0 T_0 \parallel (\Omega_a, 0) \mathcal{N}_a T_a \rangle .\end{aligned} \tag{14}$$

Here the extra 'quantum number' Ω_a, omitted in the labelling scheme discussed in the previous paragraph, is the half the total degeneracy of the level-set a,

$$\Omega_a = \frac{1}{2} \sum_{\alpha \in a} \hat{j}^2_\alpha, \quad a = 1, 2, \tag{15}$$

and labels the representations ($\omega_1 = \Omega_a, \omega_2 = 0$) of $SO(5)$ in which all particles are fully paired. More general representations, such as that characterizing the operator in (14), require two nonzero labels ω_1 and ω_2. The first factor on the right-hand side of that equation is a reduced matrix element that depends only on Ω_a and the operator quantum numbers ω_1 and ω_2. All the dependence on the initial and final number of particles in the system, the initial and final isospin and isospin projection, and the isospin and particle-number quantum numbers of the operator appear in the double-barred $SO(5)$ 'reduced Clebsch–Gordan' coefficient (which is independent of the isospin-projection quantum numbers) and an ordinary isospin Clebsch–Gordan coefficient.

The work of [22] allows one to decompose the 0ν operator M^F in (2) into operators with good $SO(5) \times SO(5)$ quantum numbers and lists some of the needed $SO(5)$ Clebsch–Gordan coefficients; the rest are constructed in [20]. The results can be summarized as follows. Define summed particle–particle and particle–hole-like matrix elements of *any* two body operator $\mathcal{M}$ that changes charge by two units—acting in the lower shell (shell 1)—as

$$\begin{aligned}\mathcal{F}^{pp} &\equiv \sum_{\alpha,\beta \in 1} \hat{j}_\alpha \hat{j}_\beta \left\langle [\alpha\alpha]^0 \middle| \mathcal{M} \middle| [\beta\beta]^0 \right\rangle \\ \mathcal{F}^{ph} &\equiv \sum_{\alpha,\beta \in 1} \sum_J \hat{J}^2 \left\langle [\alpha\beta]^J \middle| \mathcal{M} \middle| [\alpha\beta]^J \right\rangle .\end{aligned} \tag{16}$$

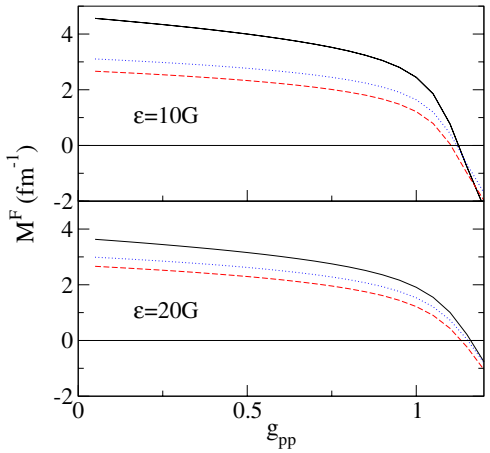

Figure 7. (After a figure in [20].) Matrix elements of Fermi 0ν operators as a function of the proton–neutron pairing strength g_{pp}. The red dashed line (- - - -) corresponds to the bare operator in the small model space and the blue dotted line ($\cdots$) to the effective operator that reproduces transitions in the two-valence-nucleon system. The black solid line (——) is the exact result in the full model space. The top and bottom panels correspond to different values of the inter-shell energy spacing ε.

These two constants completely determine, it turns out, the action of the operator $\mathcal{M}$ between any fully paired states in the lowest shell, i.e. the 'small space.' That simplicity makes for an easy and exact representation of the Lee–Suzuki mapping for two particles in the valence shells. One finds that the constants $\mathcal{F}_{\rm eff}$ for the effective Fermi $0\nu\beta\beta$ operator $M^F_{\rm eff}$—and these constants fully specify the behaviour of *that* operator in the small space—are given in terms of the $\mathcal{F}$s corresponding to the full $0\nu\beta\beta$ Fermi operator M^F by

$$\mathcal{F}^{pp}_{\rm eff} = \mathcal{F}^{pp}\frac{\langle 0_f|M^F|0_i\rangle\langle 0_f|P|0_i\rangle}{\langle 0_f|PM^FP|0_i\rangle}, \tag{17}$$

and

$$\mathcal{F}^{ph}_{\rm eff} = \mathcal{F}^{ph} + \frac{1}{2\Omega}\left(\mathcal{F}^{pp}_{\rm eff} - \mathcal{F}^{pp}\right), \tag{18}$$

where the wavefunctions $|0_i\rangle$ and $|0_f\rangle$ are the full two-neutron and two-proton ground-state wavefunctions, P projects as usual onto the 'shell-model' space (the $\mathrm{pfg}_{9/2}$ shell here), and $\Omega \equiv \Omega_1$ characterizes the size of that space. With these identifications ($\mathcal{F}$s without the subscript 'eff' are 'bare' constants), the operator $M^F_{\rm eff}$ exactly reproduces all transitions involving the lowest $\Omega(2\Omega - 1)$ states in each nucleus.

How well does this 'exact' two-body effective operator work? We illustrate the answer in figure 7, which displays the full two-shell result for the Fermi $0\nu\beta\beta$ matrix element alongside those produced by the bare operator in the truncated space and the effective two-body operator in that space. The results are plotted for two values of the level-splitting ε, and versus the proton–neutron pairing strength g_{pp}, a quantity which QRPA studies have shown to have a large effect on charge-changing matrix elements. The effective operator improves on the bare operator, particularly when $\epsilon = 20G$, where it makes up nearly half the difference between the bare and full results, but it is not anywhere near perfect. The difference between the exact and approximate results is a measure of the amount higher-body effective operators contribute

to the transitions. Such contributions, at least in this very simple and highly collective model, are quite significant.

We close this section by noting that the work of [20] can be extended in several directions. One could, with some serious effort, determine the three-body part of the effective decay operator and test whether one needs to go to four bodies for a decent result. (We certainly hope not.) And one could carry out the work just described for more complicated models, e.g. the $SO(8)$-based model discussed in [23] and [24] that includes isoscaar spin-1 pairing and a spin–isospin particle–hole force. Of course these models are not reality and so it would be hard to draw definitive conclusions from such work. But the results could be more than just suggestive.

4.2. Tests in light nuclei

In [25] tests of the Lee–Suzuki mapping at the two-body level are made in realistic systems rather than a schematic model. Realistic nearly exact calculations are only possible in light nuclei at present, and so the study concerns nuclei in the 0p shell, which do not actually double-beta decay but for which the decay matrix element can still be calculated.

The framework for the large scale nearly exact calculations is the no-core-shell model (NCSM). The authors of [25] start with two different interactions—the CD Bonn potential [26] and the N^{3}LO chiral effective-field-theory interaction [27]—and model spaces that allow between six and ten $\hbar\omega$ of excitation energy outside the p shell They first apply standard Lee–Suzuki techniques [28, 4, 29] to the Bonn potential and the similarity renormalization group (SRG) [30, 31] to the chiral potential to construct interactions appropriate for those large but not infinite model spaces. In principle the double-beta decay operator should be treated in the same way. Preliminary studies [32] showed, however, that the renormalization is slight and confined to short distances as expected, and so as in largest-scale perturbative treatments its effects are simulated through a effective Jastrow function from [17].

The small model space consists of all but four particles residing anywhere in the 0p shell and the rest forming an inert 0s-shell core. As in [33, 34], the authors first equate the effective neutron $p_{3/2}$ and $p_{1/2}$ single-particle energies to the two lowest-energy eigenvalues produced by the full calculation in ^{5}He and the effective proton energies to the corresponding eigenvalues in ^{5}Li. Then in the $A = 6$ nuclei they use the Lee–Suzuki procedure to map the two lowest $J^\pi = 0^+$ states, the lowest 1^+ state, and the two lowest 2^+ states (all with $T = 1$) onto corresponding orthogonal p-shell states. Having thus determined the two-body effective interaction (which also requires information about states with $T = 0$) and decay operator, they compare the resulting p-shell calculations of heavier nuclei with the 'exact' results.

Figure 8 presents the results for the decays ^{7,8,10}He$\rightarrow^{7,8,10}$Be when the SRG-evolved chiral N^{3}LO interaction is used in a $6\hbar\omega$ full space. The figure displays the matrix-element distributions $C(r)$ rather than simply the integrated matrix element (and there is no varying of a parameter such as g_{pp} in the algebraic model). The black (solid) curves in each of the panels denote the full-space distributions $C(r)$. These curves are what the effective operators are supposed to reproduce. The red (dashed) curves denote the result obtained with the bare $0\nu\beta\beta$ operator in the p shell, with wavefunctions produced by the effective p-shell interaction, which in turn comes from the Lee–Suzuki procedure for $A = 5$ and 6 discussed above. The blue (dot-dashed) curves are the results with the effective operator, used in conjunction with the wavefunctions from the same effective interaction.

The use of the effective decay operator clearly improves the agreement between the p-shell $C(r)$ and the full one in all three panels. One problem, however, is that $C(r)$ is not itself measurable; its integral is what we want. And it turns out that oscillations can make

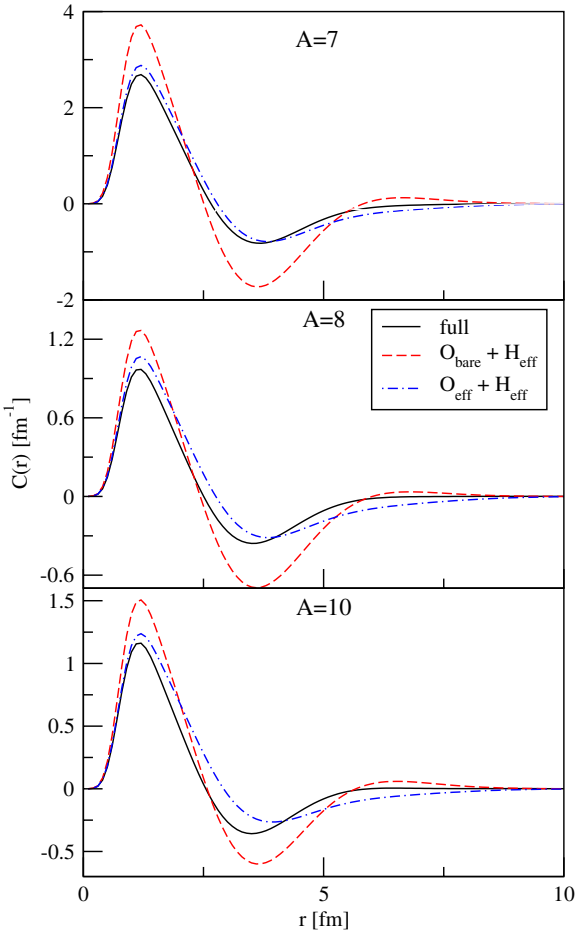

Figure 8. (From [25].) The curves $C(r)$, the integrals of which give the matrix elements for neutrinoless double-beta decay. The solid black lines (——) are the results of the full calculations with the SRG-evolved N^{3}LO potential in a $6\hbar\omega$ space, the dashed red lines (- - - -) are the results of the p-shell calculation with the effective two-body Hamiltonian and the bare decay operator, and the dot-dashed blue lines (— · —) are the results with the effective Hamiltonian and the effective decay operator. The top panel is for the decay ^{7}He $\rightarrow$ ^{7}Be, the middle panel for ^{8}He $\rightarrow$ ^{8}Be, and the bottom panel for ^{10}He $\rightarrow$ ^{10}Be.

apparent poor agreement between curves much better in the integral, and good agreement worse. Table 1 compares the matrix elements themselves for the three decays represented by the figure.

The effective operator produces a clear improvement in the integrated matrix element in $A = 7$ and (particularly) 8, but by $A = 10$ the bare operator does pretty well and the effective operator not as well. The reason is apparent from the bottom panel of figure 8: the effective-operator curve, while a better approximation than the bare curve, lies above the full curve until about $r \sim 4$ fm. The bare curve strays from the full curve at both the peak and dip but in opposite directions; it thus supplies a good approximation when integrated. Calculations with other large-space sizes and other interactions also occasionally show the same phenomenon.

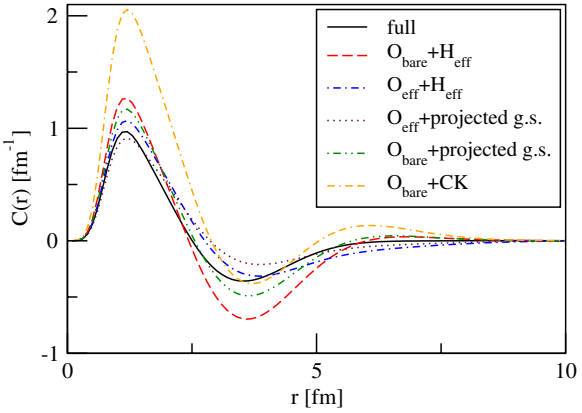

Figure 9. (After a figure in [25].) $C(r)$ for ^{8}He $\rightarrow$ ^{8}Be: the solid (black), dashed (red) and dot-dashed (blue) lines are as in the middle panel of figure 8. The dotted (maroon) and the dot-dot–dashed (green) curves result from using the normalized p-shell projections of the full ground states with the effective and the bare decay operator respectively. The dot-dashed–dashed (orange) curve is the result with bare decay operator and the CK interaction [35].

Table 1. Matrix elements $\mathcal{M}_{fi}$ produced by the distributions $C(r)$ in figure 8.

	$A = 7$	$A = 8$	$A = 10$
Full	1.76	0.48	0.79
Bare	1.49	0.18	0.91
Effective	1.90	0.59	1.23

Thus, the effective decay operator is a decided improvement but oscillations in $C(r)$ can sometimes negate its advantages. Three-body operators are clearly not negligible here, just as in the algebraic model. Although they have not yet been added to this kind of calculation, one can examine the question of whether the discrepancy at the two-body level is due mainly to the defects in the decay operator or in the interaction. If one were to carry out the Lee–Suzuki procedure in $A = 8$ and 10, the p-shell ground states would resemble the normalized p-shell projections of the full ground states. One can therefore use these normalized projections as proxies for the states that would be produced by the complete A-body Lee–Suzuki p-shell Hamiltonian. Figure 9 shows the resulting $C(r)$ with both the bare and two-body effective operators, alongside the curves already displayed in the middle panel ($A = 8$) of figure 8. The performance of the bare operator improves noticeably, so that it is about as good as the two-body effective operator in conjunction with the two-body effective Hamiltonian; its integral is $\mathcal{M}_{fi} = 0.63$. And interestingly, performance gets worse when the effective two-body operator is used with the proxy states instead ($\mathcal{M}_{fi} = 0.74$). The first result indicates that three-and-more-body terms in the Hamiltonian affect the matrix element, and the second that such terms in the decay operator do as well.

Figure 9 has one other curve, produced by the bare operator in conjunction with the phenomenological Cohen–Kurath (CK) potential [35]. One cannot really expect this empirical potential to reproduce the results of an NCSM calculation in a nucleus that is not in reality even stable, but it is nevertheless interesting to see how different its results are.

5. The future

We have seen from several points of view that a renormalization of the effective two-body decay operator improves the shell-model's ability to reproduce $0\nu\beta\beta$ matrix elements. In a very limited set of realistic perturbative calculations, this effective operator appears to improve agreement with the results of the QRPA and other kinds of calculations. But work in less realistic systems strongly suggests that three-body effective operators contribute to the matrix elements non-negligibly.

So will the two-body effective operator be sufficient in the nuclei we care about: those that actually undergo $\beta\beta$ decay? There is some reason to hope that it will perform better than it does in the light-nuclei tests just discussed. As figure 4 illustrates, the $C(r)$ curves in shell-model calculations (and QRPA calculations) in heavy nuclei nearly vanish beyond about 3 fm; there are no oscillations of consequence in those curves [36]. For that reason, the performance of the effective operator may not be degraded by the cancellations that play such a large role in the light systems. Thus, for instance, three-body diagrams in the perturbation-theoretic calculation described earlier may not alter the results as much as our simple tests suggest.

Even if they do not, however, one would ultimately like a realistic calculation that does not rely on perturbation theory, the convergence of which is difficult to ensure or estimate. There are several possible routes to that end. One promising approach is via coupled-cluster theory [37–40]. Reference [41] reports coupled-cluster calculations in ^{6}He, the first in a nucleus with two valence nucleons. Coupled-cluster techniques scale well to intermediate-mass nuclei and it should be possible to treat the nuclei ^{58}Ni, ^{58}Cu and ^{58}Zn with two nucleons in the $f_{5/2}pg_{9/2}$ shell (along with the simpler nuclei with one nucleon in that shell). Such calculations will play the same role as, e.g., the NCSM calculations discussed above, allowing the extraction of a two-body effective Hamiltonian and decay operator, which can then be used in a shell-model calculation of the decay of ^{76}Ge or ^{82}Se. And in a few years the closed-core-plus-two-nucleons that is the current coupled-cluster state of the art may be extended to closed-core-plus-three, allowing us to determine three-body effective interactions and decay operators.

Another promising approach to effective interactions is the in-medium similarity renormalization group [42, 43]. The idea is to choose a renormalization-group generator that makes the Hamiltonian increasingly block-diagonal as it evolves to lower scales; the final Hamiltonian then decouples the valence shell from the rest of the Hilbert space. Three-body interactions generated by the flow are partly included by normal ordering with respect to the nuclear core and keeping all normal-ordered two-body interactions. Thus far the procedure has been applied in open shells only to ^{6}Li and ^{18}O but it appears to work there as well or better than the most sophisticated perturbative calculations. The continued development of the approach to effective operators and valence three-nucleon terms will eventually have an impact in the field of double-beta decay.

There is promise in the future. The only question is how long it will take to realize it.

Acknowledgments

This work was supported in part by DOE grant DE-FG02-97ER41019. The crucial contributions of collaborators and coauthors G Hagen, J Holt, P Navratil, D Shukla, and P Vogel are deeply appreciated.

References

[1] Šimkovic F, Pantis G, Vergados J D and Faessler A 1999 Additional nucleon current contributions to neutrinoless double beta decay *Phys. Rev.* C **60** 055502

[2] Šimkovic F, Faessler A, Rodin V, Vogel P and Engel J 2008 Anatomy of the $0\nu\beta\beta$ *nuclear matrix elements* *Phys. Rev.* C **77** 045503
[3] Menéndez J, Gazit D and Schwenk A 2011 Chiral two-body currents in nuclei: Gamow–Teller transitions and neutrinoless double-beta decay *Phys. Rev. Lett.* **107** 062501
[4] Suzuki K and Lee S Y 1980 Convergent theory for effective interaction in nuclei *Prog. Theor. Phys.* **64** 209
[5] Navratil P and Barret B R 1998 Shell model calculations for the three-nucleon system *Phys. Rev.* C **57** 562
[6] Engel J and Hagen G 2009 Corrections to the neutrinoless double -β-decay operator in the shell-model *Phys. Rev.* C **79** 064317
[7] Ellis P J and Osnes E 1977 An introductory guide to effective operators in nuclei *Rev. Mod. Phys.* **49** 777
[8] Brandow B 1967 Linked-cluster expansions for the nuclear many-body problem *Rev. Mod. Phys.* **39** 711
[9] Machleidt R 1989 The meson theory of nuclear forces and nuclear structure *Adv. Nucl. Phys.* **19** 189
[10] Bogner S K, Kuo T T S and Schwenk A 2003 Model-independent low momentum nucleon interaction from phase shift equivalence *Phys. Rep.* **386** 1
[11] Caurier E, Menendez J, Nowacki F and Poves A 2008 The influence of pairing on the nuclear matrix elements of the neutrinoless double beta decays *Phys. Rev. Lett.* **100** 052503
[12] Miller G A and Spencer J E 1976 Pion exchange reactions with nuclei *Ann. Phys.* **100** 562
[13] Roth R, Hergert H, Papakonstantinou P, Neff T and Feldmeier H 2005 Matrix elements and few-body calculations within the unitary correlation operator method *Phys. Rev.* C **72** 034002
[14] Kortelainen M and Suhonen J 2007 Improved short-range correlations and $0\nu\beta\beta$ nuclear matrix elements of ^{76}Ge and ^{82} Se *Phys. Rev.* C **75** 051303
[15] Kortelainen M and Suhonen J 2007 Nuclear matrix elements of $0\nu\beta\beta$ decay with improved short-range correlations *Phys. Rev.* C **76** 024315
[16] Engel J 2012 *CIPANP2012: 11th Conf. on the Intersections of Particle and Nuclear Physics* https://indico.triumf.ca/contributionDisplay.py?contribId=452&sessionId=54&confId=1383
[17] Šimkovic F, Faessler A, Müther H, Rodin V and Stauf M 2009 The $0\nu\beta\beta$ -decay nuclear matrix elements with self-consistent short-range correlations *Phys. Rev.* C **79** 055501
[18] Ellis P J 1975 Calculation of other effective operators *Lect. Notes Phys.* **40** 296–312
[19] Krenciglowa E M and Kuo T T S 1975 A folded-diagram perturbation expansion for effective operators *Nucl. Phys.* A **240** 195–220
[20] Engel J and Vogel P 2004 Corrections to the neutrinoless double-beta-decay operator in the shell model *Phys. Rev.* C **69** 034304
[21] Dussel G G, Maqueda E and Perazzo R P J 1970 A two-level solvable model involving competing pairing interactions *Nucl. Phys.* A **153** 469
[22] Hecht K T 1967 Five-dimensional quasi-spin the n, T dependence of shell-model matrix elements in the seniority scheme *Nucl. Phys.* A **102** 11
[23] Engel J, Vogel P and Zirnbauer M R 1988 Nuclear structure effects in double-beta decay *Phys. Rev.* C **37** 731
[24] Engel J, Pittel S, Stoitsov M, Vogel P and Dukelsky J 1997 Neutron–proton correlations in an exactly solvable model *Phys. Rev.* C **55** 1781
[25] Shukla D, Engel J and Navritil P 2011 Nonperturbative renormalization of the neutrinoless double-beta operator in p-shell nuclei *Phys. Rev.* C **84** 044316
[26] Machleidt R, Holinde K and Elster C 1987 The Bonn meson exchange model for the nucleon nucleon interaction *Phys. Rept.* **149** 1
[27] Entem D R and Machleidt R 2002 Accurate nucleon–nucleon potential based upon chiral perturbation theory *Phys. Lett.* B **524** 93–8
[28] Okubo S 1954 Diagonalization of Hamiltonian and Tamm–Dancoff equation *Prog. Theor. Phys* **12** 603
[29] Navratil P and Barrett B R 1998 Shell-model calculations for the three-nucleon system *Phys. Rev.* C **57** 562
[30] Bogner S K, Furnstahl R J and Perry R J 2007 Similarity renormalization group for nucleon–nucleon interactions *Phys. Rev.* C **75** 061001
[31] Bogner S K, Furnshal R J, Maris P, Perry R J, Schwenk A and Vary J P 2008 Convergence in the no-core shell model with low-momentum two-nucleon interactions *Nucl. Phys.* A **801** 21–42
[32] Stetcu I 2009 private communication
[33] Lisetskiy A F, Barrett B R, Kruse M K G, Navratil P, Stetcu I and Vary J P 2008 Ab initio shell model with a core *Phys. Rev.* C **78** 044302
[34] Lisetskiy A F, Kruse M K G, Barrett B R, Navratil P, Stetcu I and Vary J P 2009 Effective operators from exact many-body renormalization *Phys. Rev.* C **80** 024315
[35] Cohen S and Kurath D 1965 Effective interactions for the 1p shell *Nucl. Phys.* A **73** 1–24
[36] Šimkovic Fedor, Faessler A, Rodin V, Vogel P and Engel J 2008 Anatomy of the $0\nu\beta\beta$ nuclear matrix elements *Phys. Rev.* C **77** 045503

[37] Crawford T D and Schaefer Henry F III 2007 An introduction to coupled cluster theory for computational chemists *Rev. Comput. Chem.* **14** 33
[38] Dean D J and Hjorth-Jensen M 2003 Coupled cluster approach to nuclear physics *Phys. Rev.* C **69** 054320
[39] Hagen G, Papenbrock T, Dean D J and Hjorth-Jensen M 2008 Medium-mass nuclei from chiral nucleon–nucleon interactions *Phys. Rev. Lett.* **101** 092502
[40] Hagen G, Papenbrock T, Dean D J and Hjorth-Jensen M 2010 Ab initio coupled-cluster approach to nuclear structure with modern nucleon–nucleon interactions *Phys. Rev.* C **82** 034330
[41] Jansen G R, Hjorth-Jensen M, Hagen G and Papenbrock T 2011 Ab initio coupled-cluster theory for open-shell nuclei *Phys. Rev.* C **83** 054306
[42] Tsukiyama K, Bogner S K and Schwenk A 2011 In-medium similarity renormalization group for nuclei *Phys. Rev. Lett.* **106** 222502
[43] Tsukiyama K, Bogner S K and Schwenk A 2012 In-medium similarity renormalization group for open-shell nuclei arXiv:1203.2515